

Learning Reward Functions for Cooperative Resilience in Multi-Agent Systems

Manuela Chacon-Chamorro

Luis Felipe Giraldo

Nicanor Quijano ^{*†‡}

Abstract

Multi-agent systems often operate in dynamic and uncertain environments, where agents must not only pursue individual goals but also safeguard collective functionality. This challenge is especially acute in mixed-motive multi-agent systems. This work focuses on **cooperative resilience**—the ability of agents to anticipate, resist, recover, and transform in the face of disruptions—a critical yet underexplored property in Multi-Agent Reinforcement Learning. We study how reward function design influences resilience in mixed-motive settings and introduce a novel framework that learns reward functions from ranked trajectories, guided by a cooperative resilience metric. Agents are trained in a suite of social dilemma environments using three reward strategies: (i) traditional individual reward; (ii) resilience-inferred reward; and (iii) hybrid that balance both. We explore three reward parameterizations—linear models, hand-crafted features, and neural networks—and employ two preference-based learning algorithms to infer rewards from behavioral rankings. Our results demonstrate that *hybrid strategy* significantly improve robustness under disruptions without degrading task performance and reduce catastrophic outcomes like resource overuse. These findings underscore the importance of reward design in fostering resilient cooperation, and represent a step toward developing robust multi-agent systems capable of sustaining cooperation in uncertain environments.

Keywords: Multi-agent systems, Inverse reinforcement learning, Preference-based learning, Reward design, Cooperative resilience, Social dilemmas.

1 Introduction

Multi-agent systems often operate in dynamic and uncertain environments, where disruptions threaten overall functionality [1, 2]. In particular, in mixed-motive multi-agent systems, agents must do more than simply optimize individual performance, they must collectively adapt and recover from disruptions to preserve system-level well-being. Disruptions, whether internal (e.g., system failures), external (e.g., environmental shocks), or adversarial (e.g., targeted attacks), can compromise system performance, underscoring the need for adaptive recovery mechanisms [1]. This motivates recent studies of resilience in multi-agent systems [3, 4], in particular the concept of **cooperative resilience**, defined as the ability of agents to sustain system-level well-being by anticipating, resisting, recovering, and transforming under disruption [3]. Unlike traditional notions of stability, equilibrium, or robustness, cooperative resilience captures the dynamic, temporal, and distributed nature of multi-agent systems operating in uncertain and failure-prone environments.

Cooperative resilience represents a critical yet underexplored dimension in Multi-Agent Reinforcement Learning (MARL). Conventional MARL methods, including value factorization approaches such as QMIX [5] and policy gradient methods such as PPO [6], rely on the specification of a coherent reward function. This reward must capture the interdependent nature of the joint task shaped by agents' interactions. However, how the reward design influences the ability of agents to cooperate, adapt, and persist under adverse conditions is still not sufficiently understood. This limitation becomes particularly evident in mixed-motive settings,

^{*}This work was supported by Google through the Google Research Scholar Program, and by the UniAndes–DeepMind Scholarship 2023.

[†]The authors are with the School of Engineering, Universidad de los Andes, Bogotá, Colombia (emails: {m.chaconc, lf.giraldo404, nquijano}@uniandes.edu.co)

[‡]This manuscript has been submitted to IEEE Transactions on Artificial Intelligence.

where agents must balance individual goals with collective outcomes, making the design of effective incentive mechanisms especially challenging [7, 8].

In this work, we address this challenge using Inverse Reinforcement Learning (IRL) [9–11], a principled framework for inferring reward functions from observed agent behavior. IRL recovers latent reward functions that are assumed to have generated trajectories exhibiting desirable or near-optimal responses to disruptions. This approach enables the discovery of incentive structures that support emergent properties such as cooperative resilience, without requiring explicit encoding of such behaviors in the reward design. This perspective is complementary to recent work on group resilience through collaboration protocols [4], which seeks to improve resilience by designing mechanisms and interaction structures that make agents more robust to perturbations. In contrast, our goal is to *infer* a reward function that captures cooperative resilience directly from behavioral evidence. Protocol-based approaches enrich agents’ capabilities, while resilience-aligned reward inference uncovers the underlying incentive structure that can support resilient collective behavior.

Building on this idea, we introduce an approach for learning reward functions from ranked agent trajectories scored with a cooperative resilience metric. This metric quantitatively evaluates how well trajectories preserve collective welfare in the presence of disruptions. By using it, we generate preference rankings over observed behaviors and feed them into a preference-based IRL pipeline to infer reward functions that implicitly encode cooperative resilience. In this way, our main contribution is a reward function design method that leverages cooperative resilience to infer a collective reward component, steering agents toward sustained system performance under disruptions. The learned reward is, in principle, compatible with different MARL algorithms, since it can be used as a drop-in replacement for the underlying reward signal. In this sense, our framework offers a flexible reward-design component that can complement existing methods.

We validate our approach in a mixed-motive social dilemma inspired by the Commons Harvest scenario from Melting Pot [12, 13]. The environment captures the tension between individual incentives to maximize resource consumption and the collective need to preserve shared resources. Our results show that resilience-inferred rewards foster adaptive behaviors under disruption, extending sustainability and improving collective outcomes compared to baselines PPO and QMIX. To assess scalability, we extended the evaluation to larger multi-agent environments with more agents and resource limitations, where our method enhanced cooperative resilience and, beyond that, improved overall system behavior by extending sustainability and collective well-being over time, without sacrificing individual task performance. This highlights our broader insight: reward functions can be treated as a form of *a priori* knowledge, extracted from trajectory analysis under a system-level cooperative resilience metric.

The remainder of this paper is organized as follows. Section 2 reviews related work, Section 3 presents our framework and Section 4 details the experimental setup and key results. Section 5 concludes with a summary and future directions. The appendix provides implementation details, extended results, and reproducibility information for experiments.

2 Background and Related Work

2.1 Cooperative AI and Resilience

Cooperative AI studies the design of multi-agent systems that achieve outcomes benefiting the group as a whole [14, 15]. In mixed-motive environments, where agents must balance individual objectives with collective welfare, designing mechanisms that foster cooperation is particularly challenging [15]. Standard reinforcement learning approaches often emphasize individual performance, which can lead to selfish behavior and the degradation of shared resources, especially in the presence of social dilemmas [8, 16–18].

The introduction of disruptions, such as resource scarcity, unsustainable behaviors, or abrupt environmental changes, further complicates cooperation [19, 20]. In these contexts, resilience becomes essential to sustain joint welfare. We focus on **cooperative resilience** [3, 21], similar to the concept of group resilience [4], a system-level property that quantifies how well a group of agents can maintain collective well-being under stress. Building on approaches from ecology, infrastructure, and economic networks [22–24], the methodology in [3] evaluates resilience by comparing disrupted vs. baseline performance across indicators of collective well-being, producing a score of this property. This score provides a quantitative basis for comparing systems

and analyzing the behaviors and incentives that lead to resilient outcomes. It can also inform the design of new agents and reward structures that promote both cooperation and robustness.

2.2 Multi-agent Reinforcement Learning

Traditional Reinforcement Learning (RL) optimizes single-agent behavior through trial-and-error, but in multi-agent settings strategic interdependence makes learning more complex, giving rise to coordination, competition, and equilibrium. To address these challenges, MARL algorithms such as QMIX [5] and COMA [25] tackle credit assignment, while social reward shaping methods [26, 27] encourage cooperation and mitigate free-riding by rewarding agents for influencing others’ actions [26]. More recent incentive-exchange mechanisms, such as peer reward [28, 29], norm formation through sanctions [30], and mutual acknowledgment protocols [31], enable agents to deliberately influence the rewards of others, thus promoting pro-social behavior through structured interactions. These methods operate by designing incentives or communication protocols that induce cooperation.

However, all of these approaches presuppose the availability of a coherent reward structure. In mixed-motive environments, this becomes particularly challenging: the reward must balance individual and collective welfare, and under disruptive conditions the relevant system-level property is *cooperative resilience*. Designing such reward functions directly is difficult. This motivates the use of inverse reinforcement learning (IRL), where rewards are *inferred* from observed behaviors rather than engineered.

2.3 Inverse Reinforcement Learning

Inverse Reinforcement Learning (IRL) is a framework for inferring reward functions from behavior [32–34]. A major limitation is its reliance on demonstrations being optimal, which is rarely true in practice [9, 35, 36]. Extending IRL to multi-agent settings (MAIRL) introduces further challenges such as joint action spaces and equilibrium-based formulations [37–39], which become intractable in complex or disrupted domains [9]. Alternatives like swarMDP [40] learn local rewards but struggle to generalize. To address this, we adopt preference-based IRL [35, 41], which learns from trajectory comparisons and is well-suited to cooperative resilience, where behaviors can be naturally ranked.

3 Problem Formulation and Methodology

We consider multi-agent environments where agents interact under mixed-motive conditions and share access to common resources. The environment is modeled using the standard *joint-state*, *joint-action* formulation of a Markov game (or multi-agent MDP), defined by the tuple (S, A, P, R, γ) , where S is the global environment state, $A = A_1 \times \dots \times A_n$ is the joint action space, P is the transition function over the joint state-action space, R denotes the reward structure, and γ is the discount factor. This formalization is consistent with the multi-agent decision-process models presented in [38, 42]. Each agent executes its own decentralized policy $\pi_i(a_i | s)$.

In this setting, standard reward functions R often prioritize short-term individual gains, which can undermine collective welfare, especially under disruptive conditions. This motivates our central objective: to learn a reward function that promotes cooperative resilience. To this end, we propose a two-step methodology: (i) ranking trajectories using a cooperative resilience metric (see Subsection 3.1), and (ii) learning a reward function from preferences using one of two methods—margin-based optimization or probabilistic modeling (see Subsection 3.2).

Figure 1 summarizes the proposed learning pipeline. The process begins with a system of interacting agents operating in a mixed-motive environment, as illustrated in panel (a). In this example setup, agents harvest resources from a shared apple tree in a grid-world, balancing individual consumption with long-term sustainability. Panel (b) presents the reward learning pipeline. First, agent trajectories are collected and evaluated using a cooperative resilience metric. This evaluation induces a ranking over trajectories based on their resilience scores. Next, this ranking is used as input to a preference-based IRL module that learns a reward function aligned with resilient behaviors. The learned reward is then integrated into the agents’ policy learning process, guiding behavior in future interactions with the environment.

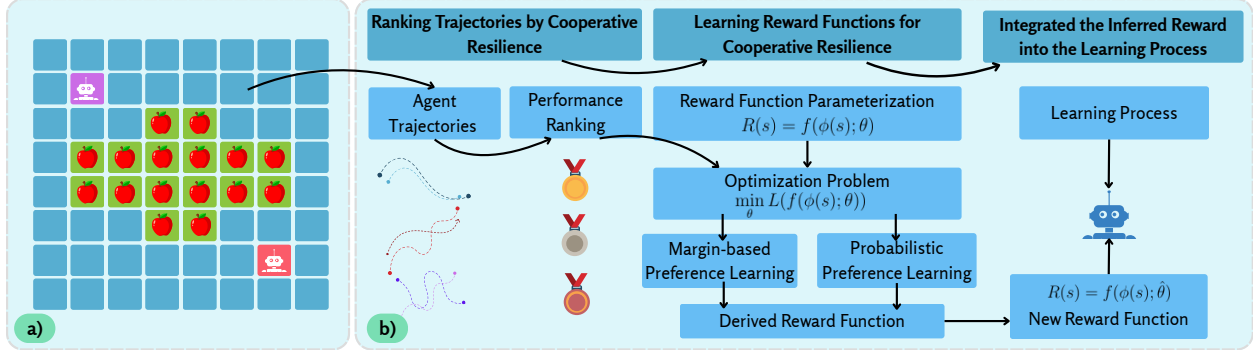


Figure 1: (a) Mixed-motive environment used throughout this study. Two agents interact in an 8×8 grid with a central apple tree containing 16 apples. (b) Overview of our proposed reward learning pipeline. This figure illustrates the full loop from data collection to policy learning.

3.1 Ranking Trajectories by Cooperative Resilience

A trajectory $\tau = (s_0, a_0, s_1, a_1, \dots, s_T)$ is defined as a sequence of states and joint actions over a time horizon T , where $s_t \in S$ and $a_t \in A$ denote the state and joint action space at time step t , respectively. Let \mathcal{D} be the set of trajectories generated by agents interacting with the environment under a given policy. We adopt the methodology from [3] to compute a resilience score $\rho(\tau)$ for each trajectory $\tau \in \mathcal{D}$. A score of $\rho = 1$ indicates alignment with a baseline without disruption, values below 1 reflect loss of resilience, and scores above 1 suggest exceptional recovery or improved performance after disruption.

To rank these trajectories, we assign a resilience score $\rho(\tau)$ to each τ . This score is based on a set of performance curves derived from four types of collective well-being indicators: **Cumulative consumption**, computed *per agent* (yielding one curve per agent); **Resource availability**, measured as the total number of apples present in the environment; **Gini index** of the consumption distribution, capturing inequality; and a **Hunger index**, estimating the delay between successive accesses to resources. The indicators we employ should be viewed as an instantiation of a more general template: the framework remains applicable as long as practitioners define the dimensions of collective well-being that matter for their particular domain.

Each indicator is measured under two conditions: a *baseline* scenario with no disruption, and a *disrupted* scenario. Let $I_k(t)$ denote the indicator k over time, t_d be the disruption time, t_f the time of worst degradation, and t_r the recovery endpoint. In practice, t_d is common to all indicators, while t_f and t_r are computed independently for each indicator to capture their distinct degradation and recovery dynamics. Consistently with [22] formulation, we set $t_f = \arg \min_{t \geq t_d} I_k^{\text{disrupted}}(t)$ within the considered window, and take t_r as either the end of the horizon (single disruption) or the last timestep before the next disruption (multiple disruptions).

We define the failure and recovery profiles as: $\text{FailureProfile}_k = \int_{t_d}^{t_f} I_k^{\text{disrupted}}(t)(I_k^{\text{baseline}}(t))^{-1} dt$, $\text{RecoveryProfile}_k = \int_{t_f}^{t_r} I_k^{\text{disrupted}}(t)(I_k^{\text{baseline}}(t))^{-1} dt$, and denote the durations $\Delta t_f = t_f - t_d$, $\Delta t_r = t_r - t_f$. Using these quantities, the resilience score for indicator k is computed as:

$$\rho_k = \frac{t_d + \text{FailureProfile}_k \cdot \Delta t_f + \text{RecoveryProfile}_k \cdot \Delta t_r}{t_d + \Delta t_f + \Delta t_r}.$$

Finally, we aggregate the indicator-specific resilience scores into a global resilience score using the harmonic mean $\rho(\tau) = \left(\frac{1}{K} \sum_{k=1}^K \frac{1}{\rho_k} \right)^{-1}$, which balances contributions across indicators by penalizing low values, thus ensuring that system resilience is not dominated by a single dimension. Ultimately, this methodology captures cooperative resilience by contrasting system behavior with and without disruption, deriving failure and recovery profiles for each indicator, and aggregating them through the harmonic mean [3].

Once the scores are computed, we induce a preference ordering over the trajectories: a trajectory τ_i is preferred over τ_j , if it exhibits a higher cooperative resilience score. Formally, the preference relationship can be expressed as $\tau_i \succ \tau_j$ if only if $\rho(\tau_i) > \rho(\tau_j)$, where $\rho(\tau)$ denotes the cooperative resilience score of

the trajectory τ . This preference structure provides the basis for learning reward functions aligned with cooperative resilience, as discussed in Subsection 3.2.

3.2 Learning Reward Functions for Cooperative Resilience

The next step is to learn a reward function $\hat{R} : S \rightarrow \mathbb{R}$ that aligns agent behavior with cooperative resilience, as indicated by the trajectory rankings. A crucial design decision at this stage is the parameterization of reward function. We assume that the reward function depends on a feature representation of the state, denoted as $\phi(s) : S \rightarrow \mathbb{R}^n$, where n is the dimensionality of the feature space. The most commonly used parameterizations include handcrafted linear functions, state-based linear functions, and nonlinear models such as neural networks.

In handcrafted linear functions, the reward is modeled as $R(s) = \phi(s)^\top w + b$, with $w \in \mathbb{R}^n, b \in \mathbb{R}$ learnable parameters, and the feature representation $\phi(s)$ is manually designed to capture properties related to the system's objective, in our case, the resilience outcome. Relevant features may include metrics such as resource availability, fairness indicators, or inter-agent distances. This approach offers high interpretability and simplicity, but heavily depends on the quality of the handcrafted features.

In state-based linear functions, the feature representation is set as $\phi(s) = s$ directly using the raw state variables. This approach removes the need for feature engineering but may struggle to capture complex relationships when resilience-relevant properties are nonlinearly entangled in the state space. Nonlinear models, such as neural networks parameterized as $R(s; \theta)$ offer greater flexibility by capturing complex, nonlinear dependencies between the state and resilience outcomes. However, they typically involve high-dimensional parameter spaces and require larger datasets and longer training processes to achieve good generalization. Moreover, the optimization landscape becomes more challenging, increasing the risk of convergence to sub-optimal local minima instead of the desired global optimum.

Once a parameterization is chosen, we formulate the preference-based learning problem using the trajectory rankings induced by cooperative resilience scores. We explore two approaches to learn a reward function from these preferences: (i) Margin-based Preference Learning (MPL), and (ii) Probabilistic Preference Learning (PPL).

3.2.1 Margin-based Preference Learning

This approach aims to learn a reward function such that more resilient trajectories accumulate higher total reward than less resilient ones. Given a pair of ranked trajectories (τ_i, τ_j) , where $\tau_i \succ \tau_j$ indicates that τ_i is more resilient than τ_j , as measured by an external cooperative resilience metric. Then the learning objective is to ensure that $\sum_{s \in \tau_i} R(s; \theta) > \sum_{s \in \tau_j} R(s; \theta)$.

To model this preference, we introduce a margin $\delta_{ij} > 0$, which can be fixed (e.g. $\delta_{ij} = 1$, as in traditional MPL) or dynamically set to reflect the resilience gap between trajectories $\delta_{ij} = |\rho(\tau_i) - \rho(\tau_j)|$.

We then formulate the optimization problem as

$$\min_{\theta} \sum_{(\tau_i \succ \tau_j)} \max \left(0, \delta_{ij} - \left(\sum_{s \in \tau_i} R(s; \theta) - \sum_{s \in \tau_j} R(s; \theta) \right) \right).$$

When $R(s; \theta)$ is a linear function of state features, this problem is convex. For nonlinear models (e.g., neural networks), the objective becomes non-convex, and the optimization must be approached using iterative methods with appropriate regularization. Another important factor in optimization is how trajectory pairs are selected, as different sampling strategies influence convergence and the type of preferences captured. We evaluated three approaches: *random*, *ranked* (adjacent in the resilience order), and *mixed* (a probabilistic combination of both). The margin-based formulation thus yields six variants, combining the two margin definitions ($\delta_{ij} = 1$ or $\delta_{ij} = |\rho(\tau_i) - \rho(\tau_j)|$) with the three sampling strategies. Full implementation details are provided in the Supplementary File Section A.4.

3.2.2 Probabilistic Preference Learning

In PPL, we define the probability that the trajectory τ_i is preferred over τ_j as a function of their cumulative rewards. The learning problem is then formulated as a maximum likelihood estimation over the observed

preferences. Equivalently, the objective can be expressed as the minimization of the negative log-likelihood:

$$\min_{\theta} - \sum_{(\tau_i \succ \tau_j)} \log \left(\frac{\exp \left(\sum_{s \in \tau_i} R(s; \theta) \right)}{\exp \left(\sum_{s \in \tau_i} R(s; \theta) \right) + \exp \left(\sum_{s \in \tau_j} R(s; \theta) \right)} \right).$$

This formulation is convex when $R(s, \theta)$ is a linear function of state features, and allows efficient optimization using standard convex solvers. Compared to MPL, this approach provides smooth gradients, which can lead to more stable convergence and better handling of noisy or uncertain rankings. However, it may be computationally more expensive due to the use of exponential operations over each trajectory pair. Data sampling strategies are analogous to MPL case (see Supplementary File Section A.4).

4 Experimental Validation

4.1 Environment Description

We evaluate our approach in a simplified version of a *social dilemma* inspired by the “Commons Harvest” scenario from the Melting Pot suite [12, 13]. The original environment is defined as partially observable. In this work, we deliberately adopt a *fully observable* variant. This is consistent with many fully observable Markov games used in cooperative and mixed-motive MARL. The environment consists of a discrete 8×8 grid where 2 agents interact and harvest resources from a shared tree containing 16 apples, located in the central region of the grid (see Figure 1). Apples grow probabilistically, with regrowth chances increasing as more apples are preserved—encouraging sustainable behavior. This creates interdependence: while agents benefit from consumption, overharvesting reduces future availability and harms collective outcomes. This setting naturally captures a **mixed-motive scenario**: agents must balance individual consumption with the long-term collective benefit of preserving the resource pool.

4.2 Trajectory Collection and Resilience-Based Ranking

To initialize the reward inference process, we collect 500 trajectories generated by agents following a random policy, each lasting 1000 steps. At timestep 500, a disruption removes apples from the central tree with fixed probability, ensuring that at least one remains so the episode can continue. These trajectories are then ranked according to their **cooperative resilience** score, computed from the indicators introduced in Subsection 3.1. The resulting ranking serves as input to the preference-based IRL algorithms described in Subsection 3.2 to infer a reward function that promotes cooperative resilience. Full details of the experimental setup and configurations are provided in the Supplementary File Section A).

Note that the cooperative-resilience score is used to construct the trajectory rankings and, as discussed later, as one of our evaluation metrics. This does not introduce direct circularity, since agents never receive the resilience score during training and are instead guided only by the inferred reward function, which is a function of the state rather than of the trajectory-level metric.

4.3 Reward Inference Configurations

Building on the trajectory ranking, we evaluate multiple reward inference configurations to determine which best support collective well-being. We consider two main approaches: (i) resilience-based, where a unique reward function \hat{R} is inferred and shared by all agents, and (ii) hybrid, where \hat{R} is combined with a consumption-based individual reward. In the hybrid setting, each agent receives a reward composed of the shared resilience term and its own consumption signal.

Both approaches are tested with three parameterizations of \hat{R} : handcrafted, state-based linear, and neural network, and two optimization methods: Margin-based Preference Learning (MPL) and Probabilistic Preference Learning (PPL). MPL yields six variants, from two margin schemes and three sampling strategies, while PPL yields three, resulting in 27 total configurations (see Supplementary File Section A.6).

The inferred rewards are injected into PPO agents, which are trained for 500 episodes of 1000 steps and evaluated under the same disruption protocol used in trajectory ranking, where a subset of apples is removed from the central tree at step 500. Figure 2 reports the metric associated with the consumption of

the last remaining resource, comparing the best configurations of each reward parameterization and both optimization approaches.

In selecting these *best* configurations, we did not rely on resilience alone. Several PPL variants achieve high resilience scores (e.g., PPL-R and PPL-K), but do so by inducing overly conservative policies with low average rewards, preserving resources at the cost of individual task performance. To avoid such undesirable behaviors, we adopted a **multi-criteria selection rule**: high resilience, high cumulative reward, low last-apple consumption, and low variance across episodes. Under this joint evaluation, the MPL–M1 Hybrid with handcrafted features consistently dominated the alternatives. We adopt this reward configuration, hereafter referred to as our ***hybrid strategy***, as the reference for comparison against baseline methods under the new disruption protocol introduced in Subsection 4.4. Supplementary File Section A.5.3 provides additional metrics and plots for all configurations.

It is important to note that our chosen *hybrid strategy* relies on a handcrafted reward parameterization. Its strong performance is partly explained by the fact that its features encode meaningful prior structure about the domain, making it the least general and the most dependent on expert knowledge. At the same time, our preference-based IRL procedure must still learn appropriate weights for these features to obtain resilient, low-selfishness behavior; without the resilience-based rankings, the same features do not automatically yield suitable policies. By contrast, the linear and neural models operate directly over the full joint state and are therefore more data-hungry; with only 500 ranked trajectories in a high-dimensional, spatially structured environment, they are likely underpowered rather than fundamentally flawed.

4.4 Evaluation Metrics and Experimental Results

We have implemented an expanded disruption protocol for evaluation, applied to agent trained with *hybrid strategy*. Evaluating algorithms under the same disruption protocol used during training may risk overfitting to known conditions, thus limiting the generalization claims of our method. To address this, the new protocol introduces three temporally distributed and qualitatively distinct disruptions, each lasting 5000 steps: (i) resource removal at step 1250, (ii) a temporary reduction in apple regrowth rate starting at step 2500, and (iii) an agent failure simulation, where one agent loses control and moves randomly from steps 3750 to 3900.

In these evaluations, we consider three baselines: a random policy, PPO with a standard reward scheme (+1 for consuming an apple, 0 otherwise), and QMIX. For QMIX, the individual reward function is also defined using the +1/0 scheme, but in practice this leads agents to converge toward regions without apples. To mitigate this, we increased the reward to +10 for consuming an apple. Using this modified reward, the trained QMIX agents were evaluated with $\epsilon = 0$ under the disruption protocol. These baselines are contrasted against our *hybrid strategy*, implemented as PPO with the resilience-informed reward learned through our method.

Figure 3 summarizes performance metrics across 500 evaluation episodes. Panel (a) shows that cooperative resilience is consistently higher for the *hybrid strategy*, with both mean and median values shifted toward the upper end of the scale relative to all baselines. Panel (b) indicates that *hybrid strategy* achieves the highest average cumulative consumption across agents, demonstrating that sustainability is attained without sacrificing productivity. Panel (c) further reveals that episode lengths are significantly extended:

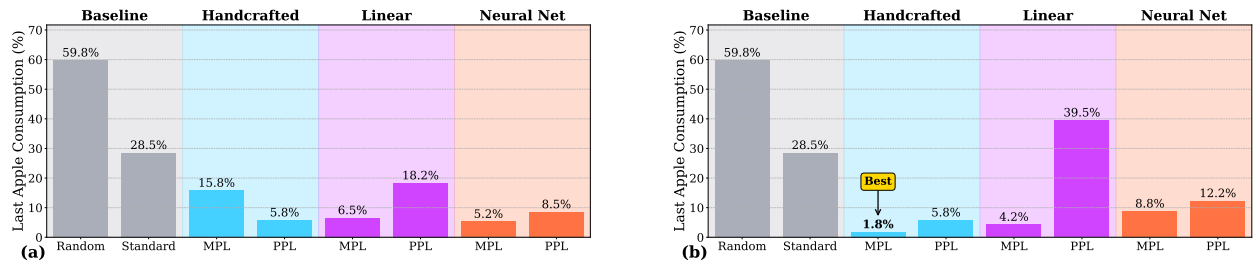


Figure 2: Percentage of episodes (out of 500) in which agents consumed the last remaining apple for the best configurations under each reward parameterization and optimization method. (a) Agents trained exclusively with resilience-aligned rewards. (b) Agents trained with *hybrid strategy*.

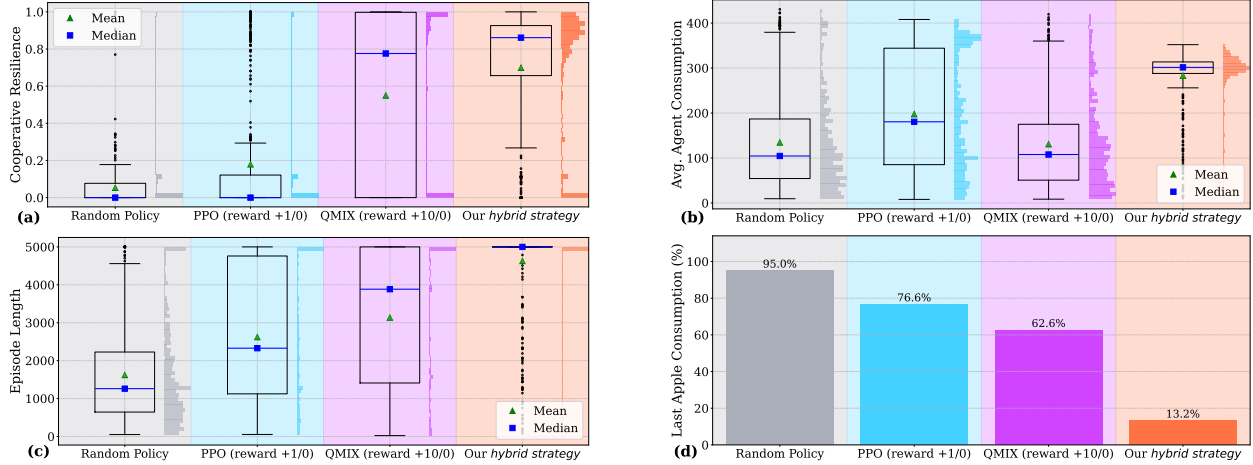


Figure 3: Performance metrics over 500 episodes. (a) Cooperative resilience. (b) Average total apple consumption per episode across both agents. (c) Episode length. (d) Last-apple consumption frequency, indicating the occurrence of social dilemma failures.

under *hybrid strategy*, resources typically remain available until the simulation horizon (5000 steps), indicating more efficient and balanced exploitation. Finally, panel (d) shows that the social dilemma of last-resource depletion is substantially mitigated: the last apple is consumed in only 13.2% of episodes.

To statistically validate these findings, we applied the Mann–Whitney U test for each metric, with p -values corrected using the Benjamini–Hochberg procedure (FDR, $\alpha = 0.05$). Bonferroni-adjusted p -values are reported in Supplementary File Section A.8.1. Results confirm that, for cooperative resilience, *hybrid strategy* significantly outperforms Random and PPO, while no significant difference is found relative to QMIX. In contrast, for both cumulative consumption and episode length, *hybrid strategy* outperforms **all** baselines after correction.

To further interpret agent behavior, we visualize the position frequency maps over 500 evaluation episodes (Figure 4). Agent 1 is shown in shades of green and Agent 2 in purple, with apple positions marked in red. Under the random policy, agents spread almost uniformly across the grid, with no clear coordination. With PPO rewards, both agents cluster in the bottom-left corner, strongly overlapping and competing for the same apples. QMIX produces an alternative but still suboptimal pattern: agents remain concentrated in the opposite corner without diversifying their movement across the grid. By contrast, the *hybrid strategy* shows a complementary specialization: Agent 1 explores a wider area, while Agent 2 remains anchored along the right boundary, harvesting resources with little movement. This emergent division of roles could avoid redundant visits and illustrates how cooperative behavior can arise from differentiated strategies. For additional visualization see Supplementary File Section C includes disaggregated position maps. These plots represent, with circles, the locations where each agent spent the most time, together with individual maps per agent to highlight their distinct spatial behaviors.

4.5 Evaluating Scalability

The initial evaluation of our approach was conducted in a simplified setting with few agents. Several extensions remain to be explored, including more complex and partially observable domains. To assess the scalability of our pipeline, we implemented a larger 16×16 grid-world with 4 agents and 3 apple trees (see Supplementary File Section A.8.2). In this environment, each tree disappears permanently once all surrounding apples are harvested, introducing a localized resource depletion mechanism and stronger interdependencies among agents. Moreover, resources can only regenerate up to a much lower threshold (16 apples in total, instead of the initial distribution), effectively limiting regrowth to the equivalent of a single tree.

We applied our full pipeline in this extended environment, including the computation of resilience indicators and reward inference using *hybrid strategy*. For reward inference, we relied on 400 ranked trajectories

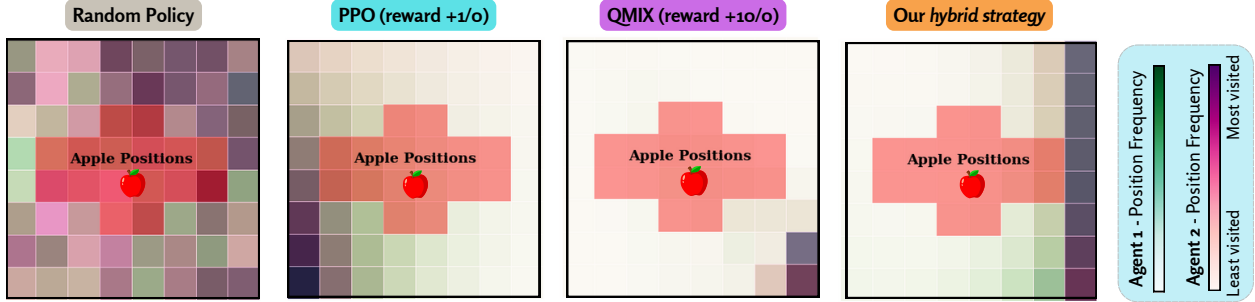


Figure 4: Position frequency maps for Agent 1 (green) and Agent 2 (purple) under four training configurations: (i) random policy, (ii) PPO with standard rewards, (iii) QMIX, and (iv) *hybrid strategy*. Each heatmap depicts the spatial visitation density over 500 evaluation episodes, with apple locations marked in red. Agents were randomly initialized at the start of each episode and evaluated under the same protocol with three disruption events.

generated from random agent behavior (see Supplementary File Section A.7). The evaluation protocol consisted of 50 episodes, each lasting 2000 steps, with a disruption introduced in 300 timestep by removing apples from the environment. In this setting, we directly transferred the *hybrid strategy* process identified in the smaller environment. Thus, the results here should be interpreted as a practical workflow in which configuration searches are performed in small environments and then the scalability of the larger ones is evaluated.

The algorithm was compared against a random policy and PPO with the traditional reward scheme. As summarized in Table 1, our *hybrid strategy* achieves higher average cooperative resilience, longer episode durations, and a reduction in social dilemma failures. To further evaluate robustness, we applied the Mann–Whitney U test with Benjamini–Hochberg corrections when comparing *hybrid strategy* against standard PPO. The results suggest that, although the improvement in average resilience is not statistically significant in this setting, resilience-based rewards during training lead to significantly longer episodes and higher cumulative rewards. These findings indicate enhanced system survivability and sustained agent performance, consistent with the intended goals of cooperative resilience. Additional results and statistical analyses for this environment are provided in Supplementary File Section A.8.2.

Table 1: Comparison of algorithms in the extended 16×16 environment with four agents.

Method	Cooperative Resilience	Apple Consumption	Episode Length	Last Apple
<i>Hybrid strategy</i>	0.889 ± 0.395	22.93 ± 4.77	1923 ± 263	6 / 50
PPO (reward +1/0)	0.814 ± 0.469	16.74 ± 4.50	1450 ± 625	25 / 50
Random policy	0.274 ± 0.293	14.51 ± 3.47	760 ± 361	50 / 50

4.6 Discussion of Results

Our experimental findings show that cooperative resilience can be improved through the proposed framework. Agents trained with the *hybrid strategy* outperform baseline policies, achieving higher cooperative resilience and more structured behaviors even when trained from random demonstrations. Incorporating individual incentives through the *hybrid strategy* preserves cooperative performance, demonstrating that individual and collective goals can be successfully aligned. Notably, the handcrafted margin-based approach offers a balance between interpretability and impact.

Under this strategy and in the evaluation protocol with three interruptions, the percentage of episodes with last-apple consumption, a proxy for selfishness, drops to only 13.2%, while maintaining apple consumption levels higher than those of the baseline methods. This confirms that agents can achieve task effectiveness while promoting fair and prosocial behavior. Moreover, spatial maps further reveal that the

hybrid strategy promotes complementary behaviors: one agent explores the environment while the other remains anchored along the boundary, consistently harvesting resources and supporting sustainability. These patterns are consistent with the handcrafted reward design, which incentivizes proximity avoidance and presence in resource-rich areas without direct competition (see Supplementary File Section B). An illustrative example is provided in the supplementary video.¹

Our comparisons are restricted to random policy, PPO and QMIX, leaving out more recent cooperative MARL baselines. Nonetheless, we emphasize that the proposed contribution is not a new MARL algorithm *per se*, but rather a reward learning framework for identifying useful incentives in mixed-motive settings. Such rewards could in principle be integrated into a wide range of existing MARL methods. Regarding scalability, we acknowledge that fully scaling to larger populations remains a central direction for future work. Scaling the framework to more complex environments will likely incur higher computational costs, suggesting caution when generalizing our findings and motivating further exploration under more realistic and scalable conditions.

5 Conclusion and Further Work

We introduced a framework for learning reward functions from ranked trajectories using a cooperative resilience metric in mixed-motive environments. By inferring a collective reward component and integrating it into MARL training, our method consistently improved system-level performance over baselines such as PPO and QMIX with traditional rewards. Agents trained with our pipeline sustained functionality under disruption, achieved longer episodes, higher cumulative consumption, and stronger cooperative resilience. Moreover, these agents developed structured spatial behaviors that reflect an alignment between incentives and collective outcomes. Scalability tests in larger environment further confirmed these benefits, underscoring the potential of our reward design as a principled approach that can complement existing MARL methods.

This work opens several directions for future research. First, extending the framework to the full version of the social dilemma environment under partial observability, as commonly encountered by agents, would provide a more realistic testbed for cooperative resilience. Future work should also explore larger and continuous state spaces, as well as adversarial settings, to evaluate the robustness of the approach under more demanding conditions. We acknowledge that fully scaling to more agents and to additional Melting Pot scenarios remains an important direction for future work. Another promising direction is to expand the set of baselines, incorporating recent cooperative MARL algorithms. Since our contribution is not a new algorithm but a method for inferring useful rewards, these inferred incentives could be integrated into diverse MARL approaches to analyze how resilience-oriented signals shape their performance.

Additionally, integrating human-generated trajectories as preference signals may offer valuable insights into natural resilience strategies, enabling the design of artificial agents that better align with human values and cooperative norms. This human-in-the-loop perspective could strengthen the applicability of cooperative resilience learning in real-world settings.

References

- [1] K. Topolewicz, S. Olaru, E. Girejko, and C. E. Dórea, “On impact of disturbance in the deployment problem of multi-agent system,” *Archives of Control Sciences*, pp. 299–320, 2023.
- [2] E. Yildirim, S. B. Sarsilmaz, A. T. Koru, and T. Yucelen, “On control of multiagent systems in the presence of a misbehaving agent,” *IEEE Control Systems Letters*, vol. 4, no. 2, pp. 456–461, 2019.
- [3] M. Chacon-Chamorro, L. F. Giraldo, N. Quijano, V. Vargas-Panesso, C. González, J. S. Pinzón, R. Manrique, M. Ríos, Y. Fonseca, D. Gómez-Barrera, and M. Perdomo-Pérez, “Cooperative resilience in artificial intelligence multiagent systems,” *IEEE Transactions on Artificial Intelligence*, 2025, to appear.
- [4] I. Shraga, G. Azran, M. Gerstgrasser, O. Abu, J. Rosenschein, and S. Keren, “Collaboration promotes group resilience in multi-agent RL,” in *Reinforcement Learning Conference*, 2025.

¹See supplementary video:
<https://drive.google.com/file/d/15j30D6HnuKYPrDJJmQVgY0yE04HSwmB3/view?usp=sharing>

[5] T. Rashid, M. Samvelyan, C. S. De Witt, G. Farquhar, J. Foerster, and S. Whiteson, “Monotonic value function factorisation for deep multi-agent reinforcement learning,” *Journal of Machine Learning Research*, vol. 21, no. 178, pp. 1–51, 2020.

[6] J. Schulman, F. Wolski, P. Dhariwal, A. Radford, and O. Klimov, “Proximal policy optimization algorithms,” *arXiv preprint arXiv:1707.06347*, 2017.

[7] Z. Nie, K.-C. Chen, and K. J. Kim, “Social-learning coordination of collaborative multi-robot systems achieves resilient production in a smart factory,” *IEEE Transactions on Automation Science and Engineering*, pp. 1–15, 2024.

[8] J. Z. Leibo, V. Zambaldi, M. Lanctot, J. Marecki, and T. Graepel, “Multi-agent reinforcement learning in sequential social dilemmas,” *arXiv preprint arXiv:1702.03037*, 2017.

[9] D. Goktas, A. Greenwald, S. Zhao, A. Koppel, and S. Ganesh, “Efficient inverse multiagent learning,” *arXiv preprint arXiv:2502.14160*, 2025.

[10] Z. Ashwood, A. Jha, and J. W. Pillow, “Dynamic inverse reinforcement learning for characterizing animal behavior,” *Advances in neural information processing systems*, vol. 35, pp. 29 663–29 676, 2022.

[11] J. Wu, W. Shen, F. Fang, and H. Xu, “Inverse game theory for stackelberg games: the blessing of bounded rationality,” *Advances in Neural Information Processing Systems*, vol. 35, pp. 32 186–32 198, 2022.

[12] J. Perolat, J. Z. Leibo, V. Zambaldi, C. Beattie, K. Tuyls, and T. Graepel, “A multi-agent reinforcement learning model of common-pool resource appropriation,” *Advances in neural information processing systems*, vol. 30, 2017.

[13] J. P. Agapiou, A. S. Vezhnevets, E. A. Duéñez-Guzmán, J. Matyas, Y. Mao, P. Sunehag, R. Köster, U. Madhushani, K. Kopparapu, R. Comanescu *et al.*, “Melting pot 2.0,” *arXiv preprint arXiv:2211.13746*, 2022.

[14] A. Dafoe, E. Hughes, Y. Bachrach, T. Collins, K. R. McKee, J. Z. Leibo, K. Larson, and T. Graepel, “Open problems in cooperative ai,” *arXiv preprint arXiv:2012.08630*, 2020.

[15] L. Hammond, A. Chan, J. Clifton, J. Hoelscher-Obermaier, A. Khan, E. McLean, C. Smith, W. Barfuss, J. Foerster, T. Gavenčiak *et al.*, “Multi-agent risks from advanced ai,” *arXiv preprint arXiv:2502.14143*, 2025.

[16] M. Rios, N. Quijano, and L. F. Giraldo, “Understanding the world to solve social dilemmas using multi-agent reinforcement learning,” *arXiv preprint arXiv:2305.11358*, 2023.

[17] I. Strümke, M. Slavkovik, and V. I. Madai, “The social dilemma in artificial intelligence development and why we have to solve it,” *AI and Ethics*, vol. 2, no. 4, pp. 655–665, 2022.

[18] S. Du, “Reimagining the future of technology: “the social dilemma” review,” *Journal of Business Ethics*, vol. 177, no. 1, pp. 213–215, 2022.

[19] J. Jasper, “A strategic approach to collective action: Looking for agency in social-movement choices,” *Mobilization: An International Quarterly*, vol. 9, no. 1, pp. 1–16, 2004.

[20] M. Orner, O. Maksimov, A. Kleinerman, C. Ortiz, and S. Kraus, “Explaining decisions of agents in mixed-motive games,” in *Proceedings of the AAAI Conference on Artificial Intelligence*, vol. 39, no. 22, 2025, pp. 23 267–23 275.

[21] M. Chacon-Chamorro, J. S. Pinzón, R. Manrique, L. F. Giraldo, and N. Quijano, “Evaluating cooperative resilience in multiagent systems: A comparison between humans and llms,” *arXiv preprint arXiv:2512.11689*, 2025.

[22] B. M. Ayyub, "Systems resilience for multihazard environments: Definition, metrics, and valuation for decision making," *Risk analysis*, vol. 34, no. 2, pp. 340–355, 2014.

[23] G. P. Cimellaro, C. Renschler, A. M. Reinhorn, and L. Arendt, "Peoples: a framework for evaluating resilience," *Journal of Structural Engineering*, vol. 142, no. 10, p. 04016063, 2016.

[24] F. Gerges, H. Nassif, X. Geng, H. A. Michael, and M. C. Boufadel, "Gis-based approach for evaluating a community intrinsic resilience index," *Natural Hazards*, vol. 111, no. 2, pp. 1271–1299, 2022.

[25] J. Foerster, "Deep multi-agent reinforcement learning," Ph.D. dissertation, University of Oxford, 2018.

[26] N. Jaques, A. Lazaridou, E. Hughes, C. Gulcehre, P. Ortega, D. Strouse, J. Z. Leibo, and N. De Freitas, "Social influence as intrinsic motivation for multi-agent deep reinforcement learning," in *International conference on machine learning*. PMLR, 2019, pp. 3040–3049.

[27] E. Hughes, J. Z. Leibo, M. Phillips, K. Tuyls, E. Dueñez-Guzman, A. García Castañeda, I. Dunning, T. Zhu, K. McKee, R. Koster *et al.*, "Inequity aversion improves cooperation in intertemporal social dilemmas," *Advances in neural information processing systems*, vol. 31, 2018.

[28] A. Lupu and D. Precup, "Gifting in multi-agent reinforcement learning," in *Proceedings of the 19th International Conference on autonomous agents and multiagent systems*, 2020, pp. 789–797.

[29] J. Yang, A. Li, M. Farajtabar, P. Sunehag, E. Hughes, and H. Zha, "Learning to incentivize other learning agents," *Advances in Neural Information Processing Systems*, vol. 33, pp. 15 208–15 219, 2020.

[30] E. Vinitsky, R. Köster, J. P. Agapiou, E. A. Duéñez-Guzmán, A. S. Vezhnevets, and J. Z. Leibo, "A learning agent that acquires social norms from public sanctions in decentralized multi-agent settings," *Collective Intelligence*, vol. 2, no. 2, p. 26339137231162025, 2023.

[31] T. Phan, F. Sommer, F. Ritz, P. Altmann, J. Nüßlein, M. Kölle, L. Belzner, and C. Linnhoff-Popien, "Emergent cooperation from mutual acknowledgment exchange in multi-agent reinforcement learning," *Autonomous Agents and Multi-Agent Systems*, vol. 38, no. 2, p. 34, 2024.

[32] S. Adams, T. Cody, and P. A. Beling, "A survey of inverse reinforcement learning," *Artificial Intelligence Review*, vol. 55, no. 6, pp. 4307–4346, 2022.

[33] A. M. Metelli, F. Lazzati, and M. Restelli, "Towards theoretical understanding of inverse reinforcement learning," in *International Conference on Machine Learning*. PMLR, 2023, pp. 24 555–24 591.

[34] S. Arora and P. Doshi, "A survey of inverse reinforcement learning: Challenges, methods and progress," *Artificial Intelligence*, vol. 297, p. 103500, 2021.

[35] D. Brown, W. Goo, P. Nagarajan, and S. Niekum, "Extrapolating beyond suboptimal demonstrations via inverse reinforcement learning from observations," in *International conference on machine learning*. PMLR, 2019, pp. 783–792.

[36] R. Poiani, C. Gabriele, A. M. Metelli, and M. Restelli, "Sub-optimal experts mitigate ambiguity in inverse reinforcement learning," *Advances in Neural Information Processing Systems*, vol. 37, pp. 85 778–85 823, 2024.

[37] S. Natarajan, G. Kunapuli, K. Judah, P. Tadepalli, K. Kersting, and J. Shavlik, "Multi-agent inverse reinforcement learning," in *2010 ninth international conference on machine learning and applications*. IEEE, 2010, pp. 395–400.

[38] M. L. Littman, "Markov games as a framework for multi-agent reinforcement learning," in *Machine learning proceedings 1994*. Elsevier, 1994, pp. 157–163.

[39] M. M. Çelikok, F. A. Oliehoek, and J.-W. van de Meent, "Inverse concave-utility reinforcement learning is inverse game theory," *arXiv preprint arXiv:2405.19024*, 2024.

- [40] A. Šošić, W. R. KhudaBukhsh, A. M. Zoubir, and H. Koepll, “Inverse reinforcement learning in swarm systems,” in *Proceedings of the 16th Conference on Autonomous Agents and MultiAgent Systems*, 2017, pp. 1413–1421.
- [41] R. Willis, Y. Du, J. Z. Leibo, and M. Luck, “Will systems of llm agents cooperate: An investigation into a social dilemma,” *arXiv preprint arXiv:2501.16173*, 2025.
- [42] C. Boutilier, “Planning, learning and coordination in multiagent decision processes,” in *TARK*, vol. 96, 1996, pp. 195–210.